Different approximations for carriers lifetimes in HgCdTe quasi-neutral regions

M. Vallone*, M. G. C. Alasio*, A. Tibaldi*†, F. Bertazzi*†, S. Hanna‡, D. Eich‡, A. Wegmann‡, H. Figgemeier‡
G. Ghione*, M. Goano*†
* Dipartimento di Elettronica e Telecomunicazioni, Politecnico di Torino, corso Duca degli Abruzzi 24, 10129 Torino, Italy
‡ AIM Infrarot-Module GmbH, Theresienstraße 2, D-74072 Heilbronn, Germany
† IEIIT-CNR, corso Duca degli Abruzzi 24, 10129 Torino, Italy
E-mail: marco.vallone@polito.it

***Abstract*—In mid- and far-infrared HgCdTe photodetectors, the maximum operating temperature is determined by the dark current, which in turn depends on charge carriers lifetimes. The ability to reduce dark current and operate at the radiative limit allows for significantly higher operating temperature, but in this new scenario some approximations, commonly and historically applied in the literature to estimate and optimize lifetimes and dark current, in some cases should be avoided.**

***Index Terms*—minority carrier lifetime, focal plane arrays, HgCdTe, dark current, diffusion current, incomplete dopants ionization**

I. Introduction

A promising material for third-generation infrared (IR) detectors is mercury cadmium telluride ($Hg_{1-x}Cd_xTe$), whose outstanding properties [1]–[3] allow to fabricate large format multi-waveband focal plane arrays (FPAs) IR detectors. HgCdTe-based heterostructures can achieve background-limited photodetection performance at near-room temperatures by using sophisticated chemical compositions and doping profiles.

Fig. 1 shows two possible architectures suitable for High Operating Temperature (HOT) detectors, pBn barrier detectors [4] and full-depleted detectors [5].

The dark current density J_{dark} receives contributions mainly from Auger and Shockley-Read-Hall (SRH) generation mechanisms. The Auger generation rate usually outweighs the SRH in quasi-neutral regions (QNR) unless the dopant concentration is greatly reduced, while in depleted regions the SRH often limits the device (for definitions of QNR and depleted regions, see [6, Ch. 1-2]). In this work, we mainly focus on the

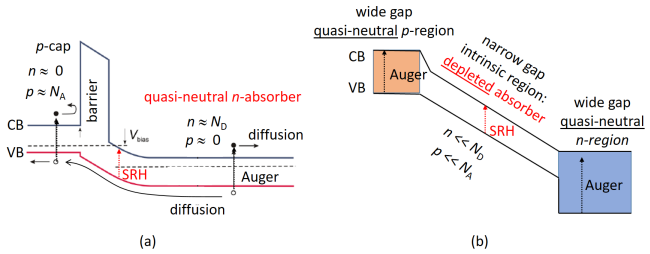

Fig. 1. (a) Qualitative band diagram of a typical pBn barrier detector [4] and (b) of a full-depleted or Auger-suppressed photodetector [5].

contribution to J_{dark} coming from the diffusion current in the QNR, i.e., charge carriers diffusing to contacts (they don't drift because there is negligible electric field surrounding them).

J_{dark} determines the maximum operating temperature and it depends on the electron and hole density n and p, both directly and through the lifetime of the minority carriers τ [7]–[10]. Thus, predicting detector performance requires calculating n and p as functions of temperature and doping, which is not a trivial issue. In this paper, we discuss some of the simplest approaches used in the literature to this end, and show that the widely used approximation which assigns the donor N_D and acceptor N_A concentrations respectively to n and p is not always appropriate.

II. Lifetime and carrier density

The SRH lifetime τ_{SRH} is connected to defect density and carrier capture cross sections [11], and it can be considered a technological parameter. The ensuing SRH diffusion current can be expressed in a simplified form as [8], [10]

$$J_{\mathrm{diff,\,SRH}} = \frac{qtn_i^2}{\tau_{\mathrm{SRH}}(n+p+2n_i)}.$$

where t is the QNR width, q is the elementary charge and n_i is the intrinsic density.

The Auger lifetimes are given by [7], [9]

$$\tau_{\mathrm{A1}} = \frac{2\tau_{\mathrm{A1}}^i n_i^2}{n(n+p)}, \quad \tau_{\mathrm{A7}} = \frac{2\tau_{\mathrm{A7}}^i n_i^2}{p(p+n)}$$

where $\tau_{\mathrm{A1,A7}}^i$ are the intrinsic A1, A7 Auger lifetimes [12]. The ensuing generation rate

$$G_{\mathrm{A}} = \frac{n_i^2}{n\tau_{\mathrm{A1}}} + \frac{n_i^2}{p\tau_{\mathrm{A7}}}$$

determines the Auger diffusion current according to [5], [8], [9], [13]

$$J_{\mathrm{diff,\,A}} = qtG_{\mathrm{A}} = qt(n+p)\left(\frac{1}{2\tau_{\mathrm{A1}}^i} + \frac{1}{2\tau_{\mathrm{A7}}^i}\right).$$

We can notice that $J_{\mathrm{diff,\,SRH}}$ decreases for increasing carrier density, whereas $J_{\mathrm{diff,\,A}}$ increases. As a result, in QNR $J_{\mathrm{diff,\,SRH}}$ can become negligible with respect to $J_{\mathrm{diff,\,A}}$ if n and/or p is large, differently from what happens in depleted regions.

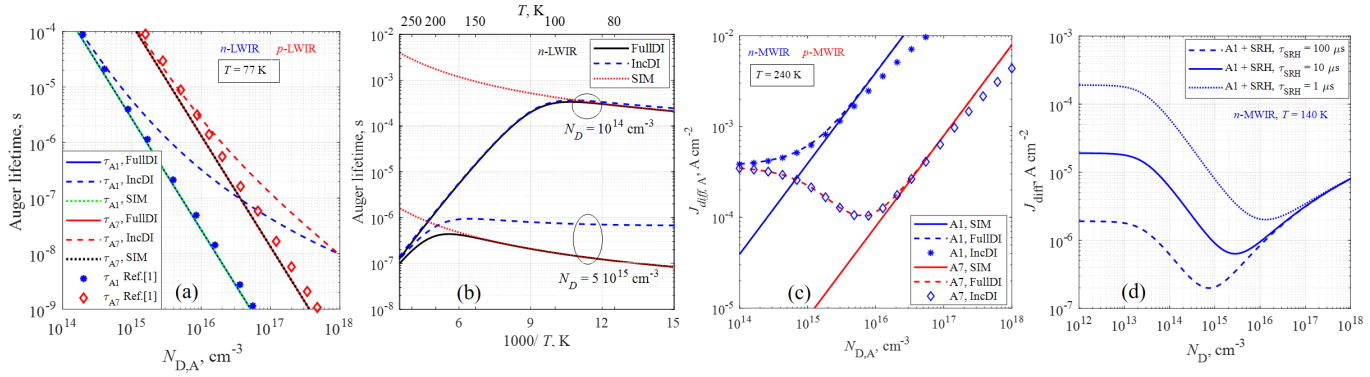

Fig. 2. (a) Auger lifetime vs. doping for n- and p-LWIR, at 77 K. Symbols are taken from [1, Fig. 3]. (b) Auger lifetime versus T for n-LWIR. (c) Auger diffusion current for n- and p-MWIR, at 240 K. (d) Total diffusion current (Auger A1 and SRH) vs. donors concentration in n-MWIR at 140 K (IncDI approximation), for three values of $\tau_{\rm SRH}$.

Lifetimes and diffusion current contributions depend on the way we calculate n and p for given N_D and N_A. Three approaches with increasing complexity can be considered: a) *simple* approximation (SIM), where it is assumed $n = N_D$ and $p = N_A$; b) the *full dopants ionization* (FullDI), where n and p follow from the mass-action $np = n_i^2$ and the electroneutrality $n + N_A = p + N_D$ equations; c) the *incomplete dopants ionization* (IncDI), where n and p are selfconsistently calculated from the electroneutrality equation $n + N_D^+ = p + N_A^-$, the Fermi levels $E_{F,n}$, $E_{F,p}$, and the ionized dopant concentrations N_A^- and N_D^+ (see definitions in [6]), with activation energies according to [14], [15].

We selected two examples of HgCdTe QNR from the literature, described in [1], [13], at equilibrium: LWIR $Hg_{1-x}Cd_xTe$, $x = 0.23$; MWIR $Hg_{1-x}Cd_xTe$, $x = 0.294$ (MWIR stands for mid-wave IR, cutoff wavelength $\lambda_c \in [3, 5]\,\mu$m, and LWIR stands for long-wavelength IR, $\lambda_c \in [8, 12]\,\mu$m).

In Fig. 2(a) the calculated Auger lifetimes are shown as functions of doping for the n- and p-LWIR at 77 K. The SIM or FullDI approximations adopted in [1] seems not the best choice for the highest doping. As for the behavior vs. temperature, Fig. 2(b) shows that the SIM approximation becomes increasingly inappropriate with increasing T and FullDI tends to deteriorate when higher doping is considered. Fig. 2(c) plots the Auger diffusion current versus dopant concentration for $T = 240$ K for a 5 μm thick n- and p-MWIR in the SIM , FullDI, and IncDI approximations.

In short, the *simple* approximation pursued e.g. in [1], [13] cannot be extended to other cases, e.g. to low-doped materials and high-T, or to high-doped materials and low-T, before having compared the obtained results with the IncDI approximation.

An interesting feature is represented by Fig. 2(d), where the total diffusion current (Auger and SRH) is plotted vs. doping for the n-MWIR QNR at 140 K. It appears that obtaining minimal dark current requires an intermediate value for N_D rather than the lowest possible doping, at least when SRH-related defect density cannot be significantly reduced, a characteristic already noticed in [13] for a very similar material.

III. Conclusions and Future Work

The performance of a detector can also be studied, at least in part, with simple models where carrier density, lifetimes and current density are expressed in closed forms, provided we use approximations within their range of validity. The interesting result shown in Fig. 2(d) deserves a deeper investigation by exploiting more sophisticated numerical simulations as in [16], which are unavoidable when dark current versus reverse bias are desired for detectors as in Fig. 1.

Acknowledgments

This work was supported in part by the European Union under the Italian National Recovery and Resilience Plan (NRRP) of NextGenerationEU, partnership on *Telecommunications of the Future* (PE00000001 – program "RESTART").

References

[1] M. A. Kinch, *et al.*, *J. Electron. Mater.* **34**, 880 (2005).
[2] M. A. Kinch, *J. Electron. Mater.* **39**, 1043 (2010).
[3] M. Reine, *J. Electron. Mater.* **44**, 2955 (2015).
[4] S. Maimon, G. W. Wicks, *Appl. Phys. Lett.* **89**, 151109 (2006).
[5] D. Lee, *et al.*, *J. Electron. Mater.* **45**, 4587 (2016).
[6] S. M. Sze, K. K. Ng, *Physics of Semiconductor Devices* (John Wiley & Sons, Hoboken, NJ, 2007), third edn.
[7] F. Bertazzi, M. Goano, E. Bellotti, *J. Electron. Mater.* **40**, 1663 (2011).
[8] M. A. Kinch, *State-of-the-Art Infrared Detector Technology* (SPIE, Bellingham, WA, 2014).
[9] P. Martyniuk, A. Rogalski, *Infrared Phys. Technol.* **70**, 125 (2015).
[10] A. Rogalski, P. Martyniuk, M. Kopytko, W. Hu, *MDPI Appl. Sci.* **11**, 501 (2021).
[11] M. Vallone, *et al.*, *J. Electron. Mater.* **44**, 3056 (2015).
[12] J. S. Blakemore, *Semiconductor Statistics*, vol. 3 of *International Series of Monographs on Semiconductors* (Pergamon Press, New York, 1962).
[13] P. Martyniuk, M. Kopytko, A. Rogalski, *Opto-Electron. Rev.* **22**, 127 (2014).
[14] A. Rogalski, *Infrared Detectors* (CRC Press, Boca Raton, FL, 2011), second edn.
[15] P. Capper, J. Garland, eds., *Mercury Cadmium Telluride. Growth, Properties and Applications* (John Wiley & Sons, Chichester, U.K., 2011).
[16] M. Vallone, *et al.*, *Appl. Opt.* **59**, E1 (2020).